

CVD Growth and Properties of Boron Phosphide on 3C-SiC

Balabalaji Padavala^a, C. D. Frye^a, Xuejing Wang^b, Balaji Raghothamachar^b, and J. H. Edgar^{a*}

^aDepartment of Chemical Engineering, Kansas State University, Manhattan, KS 66506, USA

^bDepartment of Materials Science and Engineering, Stony Brook University, Stony Brook NY 11794, USA

*Corresponding author (E-mail: edgarjh@k-state.edu)

Key words: Chemical vapor deposition, Boron phosphide, 3C-SiC, Rotational twinning, X-ray topography, Raman imaging

ABSTRACT

Improving the crystalline quality of boron phosphide (BP) is essential for realizing its full potential in semiconductor device applications. In this study, 3C-SiC was tested as a substrate for BP epitaxy. BP films were grown on 3C-SiC(100)/Si, 3C-SiC(111)/Si, and 3C-SiC(111)/4H-SiC(0001) substrates in a horizontal chemical vapor deposition (CVD) system. Films were produced with good crystalline orientation and morphological features in the temperature range of 1000 to 1200 °C using a $\text{PH}_3+\text{B}_2\text{H}_6+\text{H}_2$ mixture. Rotational twinning was absent in the BP due to the crystal symmetry-matching with 3C-SiC. Confocal 3D Raman imaging of BP films revealed primarily uniform peak shift and peak widths across the scanned area, except at defects on the surface. Synchrotron white beam X-ray topography showed the epitaxial relationship between BP and 3C-SiC was $(100)\langle 011 \rangle_{\text{BP}} \parallel (100)\langle 011 \rangle_{\text{3C-SiC}}$ and $(111)\langle 11\bar{2} \rangle_{\text{BP}} \parallel (111)\langle 11\bar{2} \rangle_{\text{3C-SiC}}$. Scanning electron microscopy, Raman spectroscopy and X-ray diffraction analysis indicated residual tensile strain in the films and improved crystalline quality at temperatures below 1200 °C. These results indicated that BP properties could be further enhanced by employing high quality bulk 3C-SiC or 3C-SiC epilayers on 4H-SiC substrates.

1. INTRODUCTION

Boron phosphide (BP) is an indirect wide-bandgap (2.0 eV) semiconductor with many outstanding properties making it attractive for various electronic device applications such as solid-state neutron detectors.[1] Bulk crystals of BP are not readily available, thus its films must be deposited on foreign substrates. In heteroepitaxy, the choice of substrate influences the morphology, crystal orientation, defect densities, impurities, and residual strain of the epitaxial layers. BP epitaxy on Si and sapphire substrates was extensively studied more than 20 years ago, but these substrates produced BP films with high concentrations of unintentional impurities and structural defects limiting its applications in electronic devices.[2–6] Other substrates are now available that may produce superior quality BP films such as SiC (4H, 6H and 3C), AlN, and ZrB₂. These materials offer better matches of lattice constants and coefficients of thermal expansion with BP, in addition to higher chemical and thermal stability compared to Si and sapphire.

3C-SiC is the most attractive SiC polytype as a substrate for BP epitaxy since both materials have the zinc-blende structure. Due to the match in crystal symmetry, 3C-SiC has the potential to eliminate in-plane rotational twinning in BP films and variations in stacking sequence at the interface. Rotational twin defects are commonly observed when the substrate material has a higher symmetry than the epilayer crystal. For example, BP(111) rotational twin defects were observed when deposited on

hexagonal substrates such as 4H-SiC(0001) and AlN(0001).[7–13] BP(111) had an index of symmetry of three whereas the (0001) plane of hexagonal substrates had an index of symmetry of six. This difference in crystal symmetry allowed two orientations of BP(111) that are related by a rotation of 180° to be deposited on the (0001) plane, leading to rotational twinning. These defects significantly contribute to the modification of electrical properties of BP, such as lifetime of minority carriers and carrier mobility. Other appealing properties of 3C-SiC as a substrate include its high thermal stability, small lattice constant mismatch (4.1%), and nearly identical coefficients of thermal expansion with BP.[14,15] 3C-SiC has a wide bandgap (2.2 eV) and high electron mobility of ~900 cm²/V·s,[16] making it suitable for making heterojunction devices with BP.

Bulk 3C-SiC single crystals with large surface areas would be ideal for growing BP films, but they are not widely available. However, large area 3C-SiC epitaxial films on silicon substrates are commercially available. These substrates are relatively inexpensive, and are available in different orientations. Past studies have shown Si contamination in BP films deposited directly on Si via autodoping and diffusion of Si atoms from Si substrate into the BP films.[1–5] Si contamination could possibly be minimized using a 3C-SiC epilayer on Si since the diffusion of Si atoms in SiC is very low at typical deposition temperatures.[17] Furthermore, 3C-SiC on 4H-SiC(0001) have been produced by Jokubavicius et al[18,19]. Such substrates can minimize Si contamination prevalent with Si substrates significantly. 3C-SiC/4H-SiC substrates have an additional advantage of enabling the deposition of BP at much higher temperatures compared to 3C-SiC/Si due to the enhanced thermal stability of 3C-SiC on 4H-SiC over Si. There are only a few prior reports of BP epitaxy on 3C-SiC in the literature. Li[20] investigated the growth of BP films on a 3C-SiC template, but epitaxy was not achieved; the film was a mixture of amorphous and polycrystalline BP. Li attributed it to the poor quality of initial 3C-SiC epilayer which was thin and non-uniform.

The present study investigated 3C-SiC templates as substrates for growing BP films over a wide range of process parameters. This paper describes the CVD growth and a detailed characterization of BP films grown on various orientations and types of 3C-SiC substrates. The effects of process variables such as temperature and reactant flow rates on the morphology, crystalline quality, residual strain and defects in the films are reported in detail.

2. EXPERIMENTAL

BP films were synthesized in a horizontal CVD reactor using ultra-high purity phosphine (99.999%) and diborane (1% in H₂) gases as phosphorus and boron precursors. The carrier gas was ultra-high purity hydrogen. Details of the CVD set-up were described in our previous work.[8,10,12,21] Three types of substrates were employed for BP deposition: 3C-SiC(100) (~4 μm) on Si(100), 3C-SiC(111) (~1 μm) on Si(111), and 3C-SiC(111) (~50 μm) on 4H-SiC(0001). The hydrogen flow rate was kept constant at 4,000 sccm, and the PH₃ and B₂H₆ (1% in H₂) flow rates were varied between 30–80 sccm and 20–80 sccm, respectively. The deposition temperature was varied between 1000 to 1200 °C over a period of 30 min to 3 h. A constant pressure of 700 torr was maintained inside the reactor chamber for all depositions.

The surface morphology of the films was characterized by scanning electron microscopy (SEM) using an FEI Versa 3D DualBeam microscope. Crystal quality of the films was analyzed by 3D Raman mapping using an Alpha300 AR+ confocal Raman imaging system (WITec Instruments Corp.) equipped with a UHTS300 spectrometer, DV970 EMCCD camera and 532 nm frequency-doubled

Nd:YAG laser as an excitation light source. 3D Raman images were acquired and analyzed using WITecControl and WITecProject Plus softwares, respectively. $\theta/2\theta$ X-ray diffraction scans were performed using a Rigaku Miniflex II desktop X-ray diffractometer with $\text{CuK}\alpha_1$ (1.54 \AA) radiation to assess the crystalline orientation of BP. High-resolution X-ray diffraction (HRXRD) double axis rocking curve scans (ω and $\omega-2\theta$) were recorded to evaluate crystalline quality and lattice strain in the BP films. The HRXRD system was equipped with a Bede D1 diffractometer with $\text{CuK}\alpha_1$ (1.54 \AA) radiation; beam conditioning was performed using Max-Flux optics and a Ge (111) monochromator. Synchrotron white beam X-ray topography (SWBXT) was used to look for rotational twinning in BP. The white beam radiation was irradiated parallel to the [100] and [111] directions of the 3C-SiC/Si substrates.

3. RESULTS AND DISCUSSION

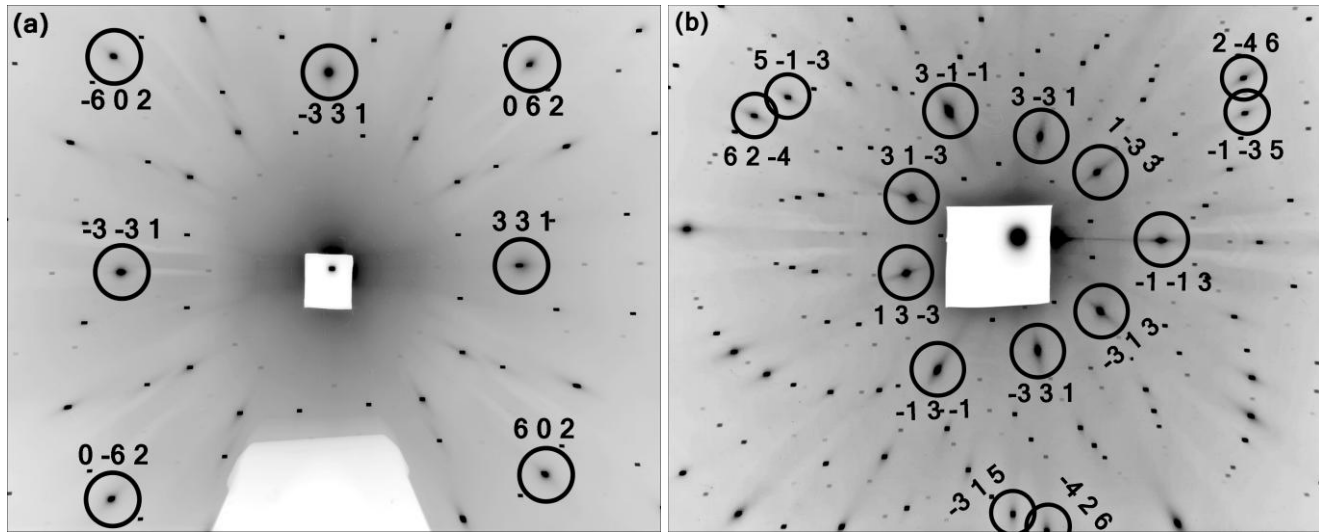


Figure 1: Indexed transmission X-ray topographs recorded on (a) 3C-SiC(100)/Si and (b) 3C-SiC(111)/Si. Spots indicated by circles represent overlapped diffraction spots from BP, 3C-SiC and Si.

Evidence of rotational twinning in BP films and the epitaxial relationship between BP and 3C-SiC/Si substrates were analyzed using SWBXT. Figures 1a and b display the 4-fold and 3-fold diffraction patterns obtained from BP films grown on 3C-SiC(100)/Si and 3C-SiC(111)/Si substrates, respectively. Diffraction spots from the zinc-blende structural layers of BP and 3C-SiC overlap completely and partially with diamond structure of Si, confirming that BP layers were epitaxially grown on both substrates. The epitaxial relationship between BP and 3C-SiC was $(100) \langle 011 \rangle_{\text{BP}} \parallel (100) \langle 011 \rangle_{\text{3C-SiC}}$ and $(111) \langle 11\bar{2} \rangle_{\text{BP}} \parallel (111) \langle 11\bar{2} \rangle_{\text{3C-SiC}}$. Also, absence of diffraction spots from the twin orientations of BP(100) and BP(111) on 3C-SiC(100) and 3C-SiC(111) substrates, respectively, confirmed that rotational twinning was eliminated. This was due to crystal symmetry matching between BP and 3C-SiC at the interface as both have same zinc-blende crystal structure. The Laue diffraction patterns recorded for BP on both 3C-SiC substrates were compared to simulated patterns to evaluate strain in the films. Diffraction spots from BP were highly elongated, confirming high residual strain in BP compared to well-defined spots from the relatively low strain 3C-SiC and high quality Si substrate. BP deposited on 3C-SiC(111)/Si demonstrated more strain than 3C-SiC(100)/Si because the spots were highly elongated on 3C-SiC(111)/Si.

3C-SiC epilayers were expected to have significant residual strain due to large lattice and thermal expansion mismatches between 3C-SiC and Si.[14,15] When BP films were deposited on the already-strained 3C-SiC, the films were also expected to demonstrate some residual strain. Confocal Raman imaging was employed to examine the residual strain and overall quality of the BP films. Raman spectra measured from BP films grown on various 3C-SiC epilayers generally gave two characteristic phonon modes: TO mode at $\sim 798 \text{ cm}^{-1}$ and LO mode at $\sim 828 \text{ cm}^{-1}$. Measured peak positions of both phonon modes were in good agreement with the previously published data.[2,8,10,12,21,22] However, a noticeable difference in peak positions was observed for BP deposited on substrates such as 3C-SiC and 4H-SiC, bulk AlN(0001), AlN(0001)/sapphire, bulk ZrB₂(0001), and ZrB₂(0001)/4H-SiC. This difference in peak positions was possibly due to residual compressive or tensile strain in the films.

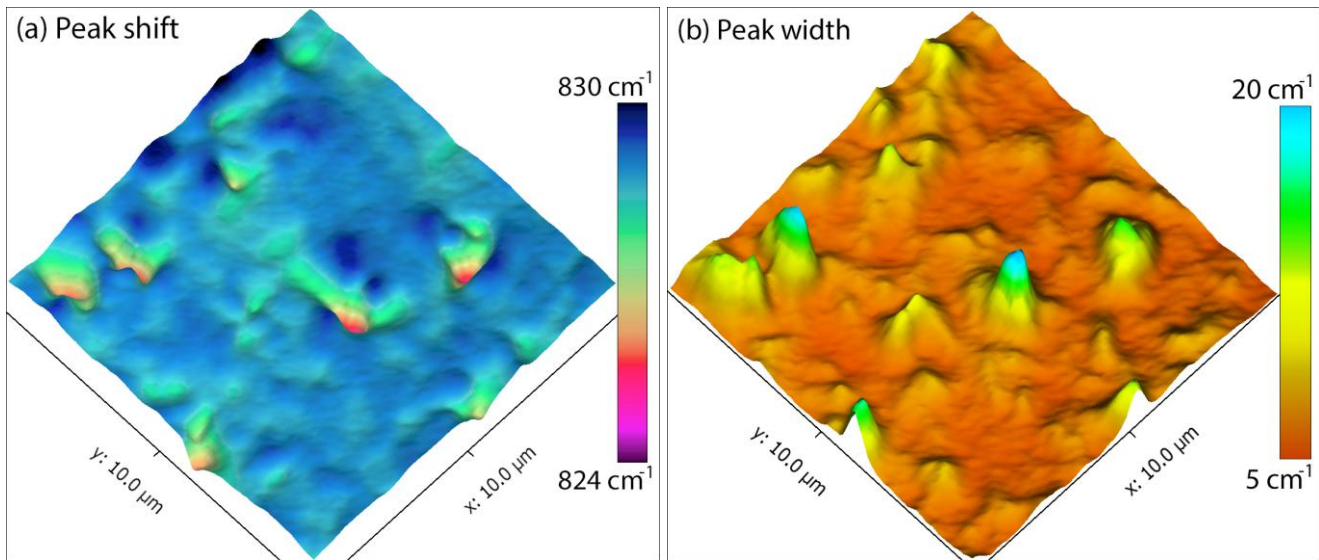


Figure 2: Raman images recorded on BP/3C-SiC(100)/Si at room temperature over an area of $10 \mu\text{m} \times 10 \mu\text{m}$ with 532 nm excitation. (a) Map of BP(LO) mode peak shift from center position; (b) Map of BP(LO) mode peak width (FWHM). Units are in cm^{-1} .

Raman spectra were collected at 10,000 points over an area of $10 \mu\text{m} \times 10 \mu\text{m}$ on BP film grown on a 3C-SiC(100)/Si substrate at 1000 °C. All data points were mapped in a 3D plot with respect to their LO phonon peak width and peak shift from center position. Raman images of peak shift and full width at half maximum (FWHM) and color scale bars are shown in Figures 2a and b. Peak shift and FWHM values were mostly uniform over the scanned area, with average values of 828.7 cm^{-1} and 6.9 cm^{-1} , respectively, with the exception of few peaks and valleys at some places. Peak positions at the deepest and highest points were 824.5 cm^{-1} and 830.5 cm^{-1} , with corresponding FWHM values of 20.5 cm^{-1} and 11.4 cm^{-1} , respectively. The overall standard deviation of peak shift and peak width was 0.50 cm^{-1} and 1.65 cm^{-1} , respectively. The huge shift in peak center position from the average value in the valleys, in particular, indicated local tensile strain in the film. Strain causes structural disorder and can change equilibrium positions of atoms in the crystal lattice, consequently shifting phonon frequencies from the film depending on the local deformation in the lattice.

An optical image of the film and scanned area for Raman imaging is shown in Figure 3a. Locations in the scanned area corresponding to valleys in the peak shift 3D map (Figure 2a) revealed huge pits in the film (shown in arrows). Several possible causes of these pits were considered including natural

surface roughness of the BP film, presence of pinhole/step bunch defects in the 3C-SiC epilayer before BP deposition, defects formed in the SiC films during BP epitaxy, or a combination of these phenomena. For more insights, the surface of a bare 3C-SiC(100) epilayer was studied by optical microscopy. Several pinholes were clearly observed on the surface, as shown in Figure 3b. Furthermore, these pinholes remain even after BP film deposition on 3C-SiC(100)/Si and 3C-SiC(111)/4H-SiC substrates, as shown in Figures 3c and d. A detailed structural characterization of these films would provide more explanation of the defects, but that characterization is beyond the scope of the present work. In summary, the significant shift in Raman peak position around the defects, which indicated strain in the BP film, could be due to a combination of factors.

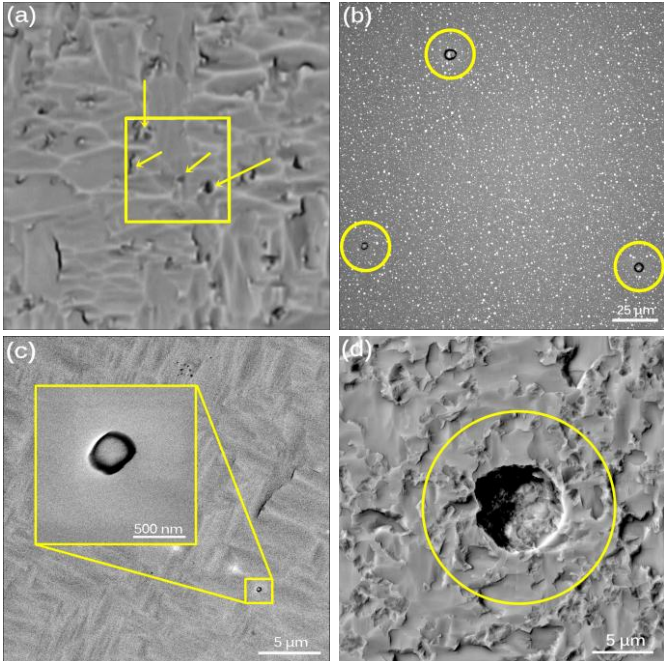


Figure 3: (a) Optical image of the BP film and scanned area ($10 \mu\text{m} \times 10 \mu\text{m}$) with Raman imaging. (b) Nomarski image of bare 3C-SiC substrate showing pinholes on surface. SEM images of BP film deposited on pinholes in (c) 3C-SiC(100)/Si and (d) 3C-SiC(111)/4H-SiC(0001) substrates

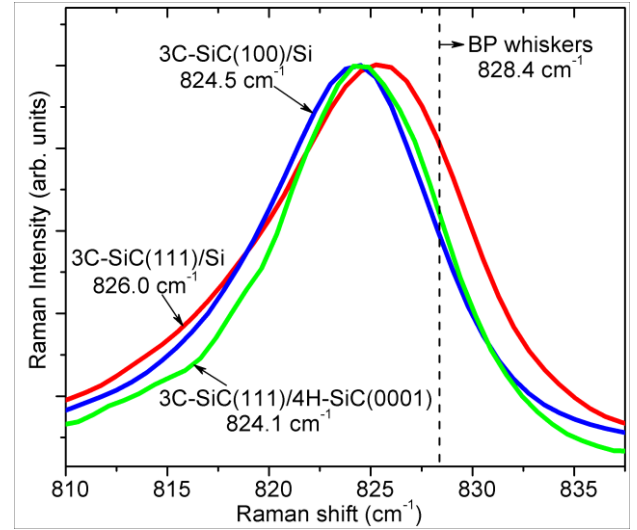


Figure 4: Comparison of Raman peak positions of BP deposited on various 3C-SiC layers to strain-free BP whiskers.

The average LO phonon peak positions of BP grown on 3C-SiC(100)/Si, 3C-SiC(111)/Si, and 3C-SiC(100)/4H-SiC(0001) at 1200°C were measured and compared to the peak positions of BP whiskers grown on 4H-SiC(0001) at 1200°C via VLS mechanism using Cr metal catalyst. BP whiskers were expected to be strain-free since these crystals freely grow outward off the substrate relaxing the strain unlike an epitaxial film, which is constrained by the substrate. The peak positions of BP films on all 3C-SiC layers were consistently lower than the peak position of strain-free BP whiskers, as shown in Figure 4. The lower shift in peak position indicated tensile strain in the BP films. The peak positions also shifted to lower wavenumbers when growth temperatures increased for a given substrate, due to increased tensile strain in the film at higher temperatures. This observation was

consistent with the trend for BP films deposited on 4H-SiC in our previous work.[10] It suggests that the coefficients of thermal expansion of substrates considered in this study are less than that of BP.

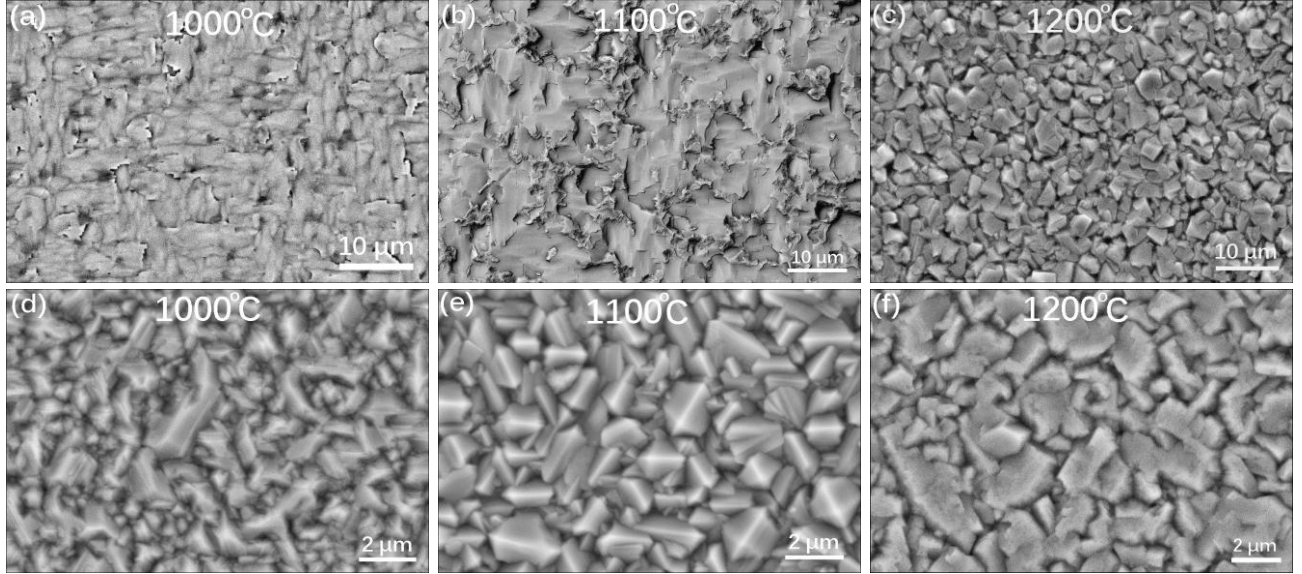


Figure 5: SEM pictures of BP films deposited on 3C-SiC(100)/Si (a, b and c) and 3C-SiC(111)/Si (d, e and f) at various temperatures.

The surface morphology of BP films deposited at various deposition conditions was analyzed by SEM and Nomarski optical microscopy (DIC). SEM micrographs of BP films grown on 3C-SiC(100)/Si and 3C-SiC(111)/Si substrates at 1000 °C, 1100 °C, and 1200 °C, respectively, are shown in Figure 5. BP films were typically dark red in color when grown at 1000 °C and 1100 °C, but they turned dark gray/black at 1200 °C. Films grown below 1200 °C had highly faceted crystallites with four-fold and three-fold symmetries representing the (100) and (111) orientations, respectively. At 1200 °C, however, a combination of regular and irregular facets grains appeared, indicating that the films were partially polycrystalline. The crystalline order of BP has been shown to improve with temperature on 4H-SiC and AlN/sapphire substrates,[8,10] but that was not the result in the present study. One probable reason for this trend could be the increased strain in films at and above 1200 °C due to large lattice and thermal expansion mismatches between BP and 3C-SiC, which inhibited the crystalline orientation of incoming atoms. BP epitaxy on a limited number of 3C-SiC(111)/4H-SiC(0001) substrates was also explored. An SEM picture of a BP film deposited at 1200 °C is shown in Figure 6. BP(111) crystallites were more faceted and had larger grain size on this substrate compared to 3C-SiC(111)/Si. The film morphology was similar to BP grown on 4H- and 6H-SiC(0001) substrates.[10]

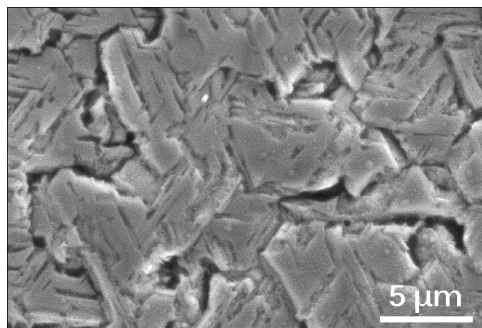


Figure 6: BP film grown on 3C-SiC(111)/4H-SiC(0001) at 1200 °C

The film thickness was measured by examining the cleaved samples in cross section by SEM. The growth rate was approximately 4-5 $\mu\text{m}/\text{hr}$. Surface roughness of a few BP films on 3C-SiC(100)/Si was measured by atomic force microscopy and are shown in Figure 7. The RMS roughness value for a film with a thickness of 3 μm , grown at 1000 °C with PH_3 and B_2H_6 (1% in H_2) flow rates of 40 sccm each, was 55 nm. When the B_2H_6 (1% in H_2) flow rate reduced from 40 sccm to 26.7 sccm, roughness of the film with a similar thickness decreased to 15 nm, due to the decreased deposition rate. In addition, orientation of BP(200) crystallites was improved when the flow rate ratio was increased. RMS roughness of BP film on 3C-SiC(100) (15 nm) was the lowest of the other substrates used, including 4H-SiC (36 nm) and AlN/sapphire (27 nm), at identical deposition conditions.

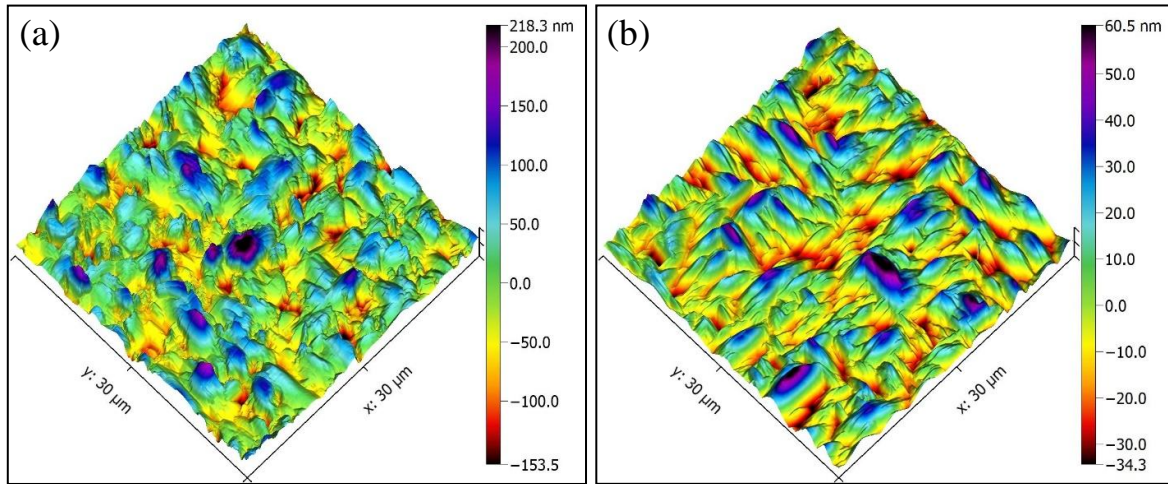


Figure 7: AFM images of BP films deposited on 3C-SiC(100)/Si at 1000°C with $\text{PH}_3/\text{B}_2\text{H}_6$ flow ratios of (a) 100 and (b) 150

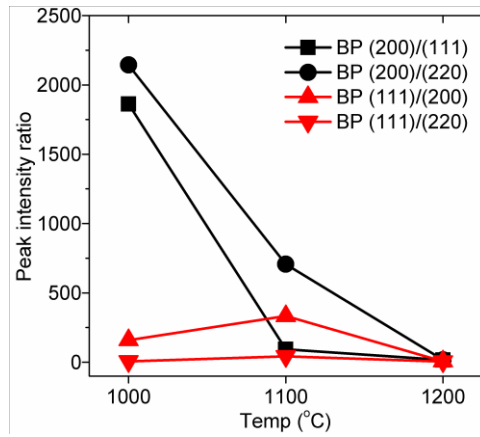


Figure 8: 0/20 XRD relative peak intensity ratios of BP deposited at various temperatures on 3C-SiC(100)/Si (black lines) and 3C-SiC(111)/Si (red lines) substrates.

The crystalline orientation of BP films on Si-base substrates was evaluated using X-ray diffraction 0/20 scans by comparing the peak intensities of preferred BP orientations to other unwanted BP orientations. The relative peak intensity ratios of BP films grown on 3C-SiC(100)/Si and 3C-SiC(100)/Si substrates at three temperatures are shown in Figure 8 indicated by black and red lines, respectively. For BP on 3C-SiC(100) layers, intensity ratios of (200)/(111) and (200)/(220) were

highest at 1000 °C, but those ratios decreased sharply with temperature up to 1200 °C. BP(111) was the preferred orientation on 3C-SiC(111)/Si substrate, and so the intensity ratios of (111)/(200) and (111)/(220) were determined. Peak ratios on the 3C-SiC(111) substrate initially increased in the temperature range of 1000 to 1100 °C, but they gradually decreased to the lowest ratio values at 1200 °C, indicating multiple BP orientations. These results were consistent with SEM findings that films deposited at 1200 °C were polycrystalline. Based on the surface morphology and XRD intensity ratios, optimum growth temperatures on 3C-SiC(100)/Si, 3C-SiC(111)/Si and 3C-SiC(111)/4H-SiC(0001) substrates were determined to be 1000 °C, 1100 °C and 1200 °C, respectively.

Table 1. FWHM and strain in BP films deposited at various conditions on 3C-SiC/Si substrates

Substrate	Growth temp (°C)	PH ₃ /B ₂ H ₆ flow ratio	ω FWHM (arcsec)	$\omega-2\theta$ FWHM (arcsec)	Theoretical mismatch (%)	Measured mismatch (%)	Out-of-plane strain (%)
3C-SiC(100)/Si	1000	100	1228	761	4.09	4.09	-0.22
	1000	150	1140	748		4.11	0.34
	1100	100	2788	949		4.12	0.46
	3C-SiC(111)/Si	1000	4041	1088		3.71	-9.42

HRXRD double-axis rocking curves were measured to estimate the film quality and lattice strain in BP films. The FWHM of ω and $\omega-2\theta$ rocking curves and lattice strain with respect to BP(100) and BP(111) at various growth conditions are given in Table 1. Peak widths of ω and $\omega-2\theta$ rocking curves decreased when PH₃/B₂H₆ flow ratio increased from 100 to 150 at 1000 °C. However, at 1100 °C with similar PH₃/B₂H₆ flow rates, the peak width and out-of-plane strain values increased significantly. As expected, the FWHM and strain values on the 3C-SiC(111)/Si substrate were significantly higher than 3C-SiC(100)/Si substrate at identical temperatures and reactant flow rates since 3C-SiC(111) films are more strained than 3C-SiC(100) films on a Si substrate. In general, the 3C-SiC epilayer has a large lattice constant mismatch and a higher thermal expansion coefficient than the Si substrate.[14,15] Thus, the 3C-SiC films are under tensile strain after cooling from the growth temperature to room temperature.[23–25] BP films on 3C-SiC(100)/Si and 3C-SiC(111)/Si substrates cracked occasionally as they were deposited on a strained 3C-SiC layer on Si. Cracking was more pronounced at high temperatures (1200 °C). Interestingly, BP films on 3C-SiC(111)/4H-SiC up to a thickness of ~6 μm did not crack, even at 1200 °C. Although Raman and HRXRD results showed tensile strain on 3C-SiC(111)/4H-SiC, BP films usually did not crack due to the very small lattice constant and thermal expansion mismatches between 3C-SiC and 4H-SiC.

4. CONCLUSIONS

BP epitaxial films with good crystalline orientation and morphological features were produced on (100) and (111) planes of 3C-SiC epilayers. Rotational twinning in BP was eliminated by depositing it on a crystal symmetry-matched 3C-SiC. Raman imaging revealed uniform peak shift and peak widths, except at defects on the film surface. Raman peak positions of BP on all types of 3C-SiC layers shifted to the lower side, indicating tensile strain in the films. The XRD pattern showed BP(100) and BP(111) to be major orientations on 3C-SiC(100) and 3C-SiC(111). HRXRD rocking curves indicated more strain in BP deposited on 3C-SiC(111)/Si than 3C-SiC(100)/Si. Due to preexisting strain in the 3C-SiC epilayer, BP films on 3C-SiC(100)/Si and 3C-SiC(111)/Si substrates cracked at high deposition

temperatures but stayed intact on 3C-SiC(111)/4H-SiC. These results suggest that either high-quality bulk 3C-SiC or 3C-SiC epilayers on 4H-SiC are the substrates for BP epitaxy, as they will produce better quality films than on silicon-based substrates.

ACKNOWLEDGEMENTS

This research was funded by the U.S. Department of Energy (DOE) under grant no. GEGF001846. We are grateful to WITec-Instruments, Knoxville, Tennessee, for generously helping us with the Raman imaging analysis of our samples. X-ray topography work was supported by the DOE, Office of Science, Office of Basic Energy Sciences, under Contract No. DE-AC02-98CH10886. X-ray topographs were recorded at beamline X19C, National Synchrotron Light Source, Brookhaven National Laboratory. We are thankful to Dr. Rositsa Yakimova and her group for providing us with 3C-SiC(111)/4H-SiC(0001) substrates for BP film depositions. We thank Dr. Bret N. Flanders for helping us with Raman spectroscopy analysis.

REFERENCES

- [1] Y. Kumashiro, Refractory semiconductor of boron phosphide, *J. Mater. Res.* 5 (1990) 2933–2947. doi:10.1557/JMR.1990.2933.
- [2] Y. Kumashiro, Y. Okada, H. Okumura, Isotope effects on boron phosphide single-crystal wafers, *J. Cryst. Growth.* 132 (1993) 611–613. doi:10.1016/0022-0248(93)90090-J.
- [3] J. Ohsawa, T. Nishinaga, S. Uchiyama, Si contamination in epitaxial boron monophosphide, *Jpn. J. Appl. Phys.* 17 (1978) 1579–1586.
- [4] T. Takenaka, M. Takigawa, K. Shohno, Diffusion layers formed in Si substrates during the epitaxial growth of BP and application to devices, *J. Electrochem. Soc.* 125 (1978) 633. doi:10.1149/1.2131514.
- [5] C.J. Kim, K. Shono, Deviation from stoichiometry of boron monophosphide, *J. Electrochem. Soc.* 131 (1984) 120–2.
- [6] E. Schrotten, A. Goossens, J. Schoonman, Photo- and electroreflectance of cubic boron phosphide, *J. Appl. Phys.* 83 (1998) 1660. doi:10.1063/1.366881.
- [7] T. Udagawa, M. Odawara, G. Shimaoka, High-resolution TEM characterization of MOVPE-grown (111)-BP layer on hexagonal 6H (0001)-SiC, *Appl. Surf. Sci.* 244 (2005) 285–288. doi:10.1016/j.apsusc.2004.10.129.
- [8] B. Padavala, C.D. Frye, X. Wang, Z. Ding, R. Chen, M. Dudley, et al., Epitaxy of Boron Phosphide on Aluminum Nitride(0001)/Sapphire Substrate, *Cryst. Growth Des.* 16 (2016) 981–987. doi:10.1021/acs.cgd.5b01525.
- [9] T.L. Chu, J.M. Jackson, A.E. Hyslop, S.C. Chu, Crystals and epitaxial layers of boron phosphide, *J. Appl. Phys.* 42 (1971) 420–4. doi:10.1063/1.1659614.
- [10] B. Padavala, C.D. Frye, Z. Ding, R. Chen, M. Dudley, B. Raghothamachar, et al., Preparation, properties, and characterization of boron phosphide films on 4H- and 6H-silicon carbide, *Solid State Sci.* 47 (2015) 55–60. doi:10.1016/j.solidstatesciences.2015.03.002.
- [11] M. Odawara, T. Udagawa, G. Shimaoka, Morphological investigation of double positioning growth of (1 1 1)-boron phosphide (BP) on the (0 0 0 1)-GaN, *Appl. Surf. Sci.* 244 (2005) 289–292. doi:10.1016/j.apsusc.2004.10.147.
- [12] B. Padavala, C. Frye, J.H. Edgar, Z. Ding, R. Chen, M. Dudley, et al., Crystal Growth and

- Characterization of Cubic Boron Phosphide on Silicon Carbide, in: Mater. Sci. Technol., 2014: pp. 1575–1582.
- [13] G. Li, J.K.C. Abbott, J.D. Brasfield, P. Liu, A. Dale, G. Duscher, et al., Structure characterization and strain relief analysis in CVD growth of boron phosphide on silicon carbide, Appl. Surf. Sci. 327 (2015) 7–12. doi:10.1016/j.apsusc.2014.11.037.
 - [14] G.A. Slack, S.F. Bartram, Thermal expansion of some diamondlike crystals, J. Appl. Phys. 46 (1975) 89. doi:10.1063/1.321373.
 - [15] R.R. Reeber, K. Wang, Lattice Parameters and Thermal Expansion of Important Semiconductors and Their Substrates, MRS Proc. 622 (2000) T6.35.1–6. doi:10.1557/PROC-622-T6.35.1.
 - [16] W.E. Nelson, F.A. Halden, A. Rosengreen, Growth and Properties of β -SiC Single Crystals, J. Appl. Phys. 37 (1966) 333. doi:10.1063/1.1707837.
 - [17] J.B. Casady, R.W. Johnson, Status of silicon carbide (SiC) as a wide-bandgap semiconductor for high-temperature applications: A review, Solid. State. Electron. 39 (1996) 1409–1422.
 - [18] V. Jokubavicius, G.R. Yazdi, R. Liljedahl, I.G. Ivanov, R. Yakimova, M. Syväjärvi, Lateral Enlargement Growth Mechanism of 3C-SiC on Off-Oriented 4H-SiC Substrates, Cryst. Growth Des. 14 (2014) 6514–6520. doi:10.1021/cg501424e.
 - [19] V. Jokubavicius, G.R. Yazdi, R. Liljedahl, I.G. Ivanov, J. Sun, X. Liu, et al., Single Domain 3C-SiC Growth on Off-Oriented 4H-SiC Substrates, Cryst. Growth Des. 15 (2015) 2940–2947. doi:10.1021/acs.cgd.5b00368.
 - [20] G. Li, Growth and properties of boron phosphide films on silicon carbide, The University of Tennessee, Knoxville, 2013..
 - [21] B. Padavala, C. Frye, J.H. Edgar, Z. Ding, R. Chen, M. Dudley, et al., Heteroepitaxial Growth of Boron Phosphide on 3C-SiC/Si(100) and AlN/Sapphire(0001) Substrates, in: Mater. Sci. Technol., 2014: pp. 1583–1590.
 - [22] J.O. Schmitt, L.J.H. Edgar, L. Liu, R. Nagarajan, T. Szyszko, S. Podsiadlo, Close-spaced crystal growth and characterization of BP crystals, Phys. Status Solidi C Conf. Crit. Rev. 2 (2005) 1077–1080.
 - [23] R. Anzalone, M. Camarda, C. Locke, J. Carballo, N. Piluso, G. D'Arrigo, et al., Stress evaluation on hetero-epitaxial 3C-SiC film on (100) Si substrates, Mater. Sci. Forum Vols. 717-720 (2012) 521–524.
 - [24] A.A. Volinsky, G. Kravchenko, P. Waters, J.D. Reddy, C. Locke, C. Frewin, et al., Residual Stress in CVD-grown 3C-SiC Films on Si Substrates, Mater. Res. Soc. Symp. Proc. 1069 (2008) D03–05.
 - [25] H. Mukaida, H. Okumura, J.H. Lee, H. Daimon, E. Sakuma, S. Misawa, et al., Raman scattering of SiC: Estimation of the internal stress in 3CSiC on Si, J. Appl. Phys. 62 (1987) 254–257.